DINAME 2023 - Proceedings of the XIX International Symposium on Dynamic Problems of Mechanics,
A.S. De Paula, A.T. Fabro and M.R. Machado (Editors), ABCM.
Pirenópolis, Go, Brazil, February 26th to March 3rd, 2023

Nonlinear dynamics of vertical axis washing machines with uncertain unbalance

Gustavo Wagner[1], **Roberta Lima**[1], **and Rubens Sampaio**[1]

[1] Department of Mechanical Engineering, PUC-Rio, Rua Marquês de São Vicente, 225, Gávea - Rio de Janeiro, RJ - Brasil - 22451-900

Abstract: A washing machine is a household appliance that has an interesting dynamical behavior, which can be well described by a set of nonlinear differential equations. When analyzing the dynamics of a washing machine, the steady state motion is an important response to consider and can be evaluated as a solution of a periodic boundary-value problem. The unbalance generated by the unevenly distribution of clothes during centrifuge is highly random and, therefore, a stochastic model is necessary to take this characteristic into account. This paper focuses on the analysis of a washing machine dynamics considering the uncertainty in the unbalance. Therefore, a stochastic model is proposed for the dynamics of a washing machine. The steady state solutions are calculated using the Shooting method combined with a sequential continuation. The probability distributions of the washing machine vibration at different spin speeds are approximated using Monte Carlo simulations. The impact of the random unbalance in the vibration amplitude of the washing machine is also investigated.

Keywords: Nonlinear dynamics, Washing machine, Shooting method, Monte Carlo simulation

INTRODUCTION

Washing machines are considered nowadays an essential household appliance. They can be divided in two main categories: vertical or horizontal axis washing machines. Although the European market is composed almost exclusively by horizontal axes washing machines, the vertical ones are still dominant in the Latin America, Middle East and South East Asia. When considering only the main global manufacturers, all the vertical axis washing machines in currently production are of the hang-suspension type. An illustrative drawing of this type of washing machine is presented in the Fig. 1, where its main components are highlighted. When considering the dynamics of washing machines, the analysis is usually restricted to a particular assemble of components called Washing Group (WG). A WG is composed by a hydraulic balancer, a drum, a tank and a drivetrain, and it is connected through a hang-suspension system to the cabinet of the washing machine.

This paper deals with the stochastic nonlinear dynamics (Cursi and Sampaio, 2015) of a WG during centrifuge stage. The dynamics is interesting and complex, mostly because of the non-usual suspension systems, that allows large displacements and rotations of the WG, the spinning of the rotating parts, that generates gyroscopic effects, and the hydraulic balancer, that passively compensates part of the unbalance in the machine. When analyzing the dynamics of a WG, the random nature of the unbalance mass of clothes adds some significant difficulty. At each new washing cycle, the pieces of clothes move randomly during the washing phase and therefore become unevenly distributed around the drum during centrifuge. This uneven distribution generates a random unbalance mass, and therefore, must be incorporated in the model as random variables. Surprisingly, as far as the authors know, all the publications about the dynamics of vertical axis washing machines have considered the unbalance mass as a deterministic quantity, which is unrealistic. The first dynamic model of hang-suspension washing machines was proposed by Conrad and Soedel (1995) and corresponds to a rudimentary model that was used to study the problem of oscillatory walk. Bae *et al.* (2002) proposed a new dynamic model of a WG in which the hydraulic balancer was considered, but assuming only small rotations. Chen and Zhang (2010) proposed a new model assuming finite rotation and analyzed the stability of the solutions, but without considering the existence of a hydraulic balancer. Later, Chen *et al.* (2011) incorporated the hydraulic balancer into the model and studied a new method for getting a smaller deflection angle. In this paper, the main contribution consists in analyze the dynamics of a WG using a stochastic model (Lima and Sampaio, 2018), so that the random nature of the unbalance is taken into account. With this analysis, it is possible to investigate the impact of the uncertain unbalance in the dynamics of the WG, which is crucial to improve the reliability of new components during product development. The dynamics of this stochastic model is analyzed in here through the computation of probability distributions of the WG's vibration (peak-to-peak amplitude) at different spin speeds. From those distributions of vibration levels, which considers the uncertainty in the unbalance parameters, it becomes possible to, for example, have a more precise procedure to evaluate the fatigue damage of the components. Also, it allows a proper set of gaps in the product to avoid possible impacts between the WG and the washing machine cabinet during centrifuge.

This paper is organized as follows. First, the deterministic nonlinear equation of motion of the WG proposed by Chen *et al.* (2011) is presented. Then, two random variables that characterize the random unbalance are incorporated to the dynamic model, transforming it from a deterministic model into a stochastic one. Then, a periodic boundary-

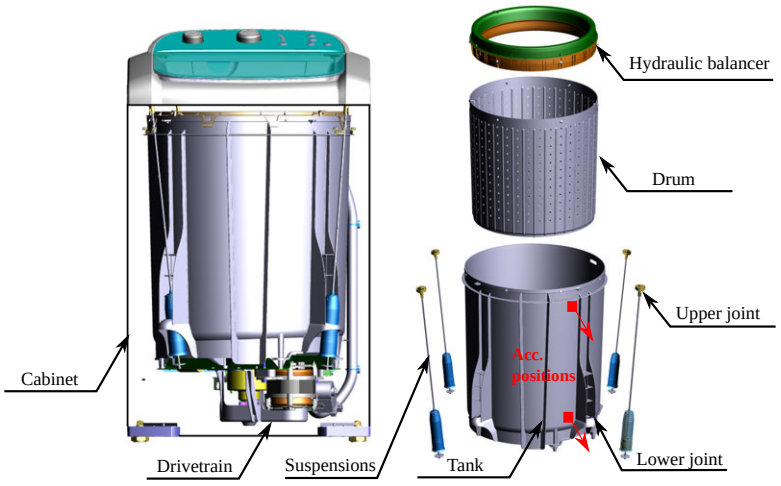

Figure 1 – Illustration of a hang-suspension vertical axis washing machine.

value problem is created to evaluate the dynamic responses at steady state condition (constant spin speeds). The Shooting method is used to evaluate periodic responses numerically, and it is combined with a sequential continuation to evaluate the periodic solutions at predefined and discrete spin speeds. Monte Carlo simulations are then performed based on samples of the probability distribution of the unbalance random variables, allowing an estimation of the probability distribution of the WG vibration. Finally, some analyses of the results are made, followed by some conclusions.

EQUATION OF MOTION

The equation of motion applied here to describe the WG dynamics was first presented by Chen *et al.* (2011), and it was derived using a Lagrangian approach. In this model, it is assumed that all the components of the WG are rigid bodies, that the upper joints of the suspension system can not translate with respect to an inertial frame, and the suspension rods can not spin. Also, the inertial forces of the suspension's rods are neglected because of their small masses. Since this model describes the WG dynamics during centrifuge, it is assumed that all water from the washing phase have been drained out, leaving in the drum only wet clothes. A additional simplification of constant inertial parameter for the clothes are used.

To evaluate the equation of motion, two reference frames were used: $X_rY_rZ_r$, which is an inertial frame fixed to the ground, and $X_bY_bZ_b$, which is a local frame embedded in the tank. The X_b and Y_b axes are located in the plane that crosses all the lower spherical joints, and the Z_b axis is equal to the axis of rotation of the drum with respect to the tank. Both frames are schematically presented in Figure 2. The random unbalance mass is not considered in this first deterministic model. Later, the unbalance mass is added to the model using tw random variables, transforming the deterministic model into a stochastic one.

Deterministic model

Following the model proposed by Chen *et al.* (2011), the equation of motion of the WG can be written as

$$(\mathbf{M}+\Delta\mathbf{M})\,\ddot{\mathbf{q}} = \frac{1}{2}\left[\frac{\partial \mathbf{M}}{\partial \mathbf{q}}\dot{\mathbf{q}}\right]^T \dot{\mathbf{q}} - \dot{\mathbf{M}}\dot{\mathbf{q}} + \mathbf{F}\left(\dot{\theta},\ddot{\theta}\right) + \mathbf{Q} + \mathbf{L} - \frac{\partial V_{WG}}{\partial \mathbf{q}}, \tag{1}$$

where $\mathbf{q} = \begin{bmatrix} x & y & z & \alpha & \beta & \gamma \end{bmatrix}^T \in \mathbb{R}^6$ corresponds to the vector of generalized coordinates and it defines the position and orientation of the local frame with respect to the inertial frame. The matrices $\Delta\mathbf{M}$ and $\mathbf{M} \in \mathbb{R}^{6\times 6}$ correspond to the mass matrix of the hydraulic balancer and the mass matrix of the rest of the WG's components, respectively. The vector $\mathbf{F}\left(\dot{\theta},\ddot{\theta}\right) \in \mathbb{R}^6$ collects all the terms related to the spin speed $\dot{\theta}$ and spin acceleration $\ddot{\theta}$ of the drum. Vectors $\mathbf{Q}$ and $\mathbf{L} \in \mathbb{R}^6$ represent the generalized forces from the suspension system and from the hydraulic balancer, respectively. At last, V_{WG} represents the gravitational potential energy of the system. Any dot superscript represents a time derivative. Interested readers should resort for Chen and Zhang (2010) and Chen *et al.* (2011) for the complete derivation of this equation of motion.

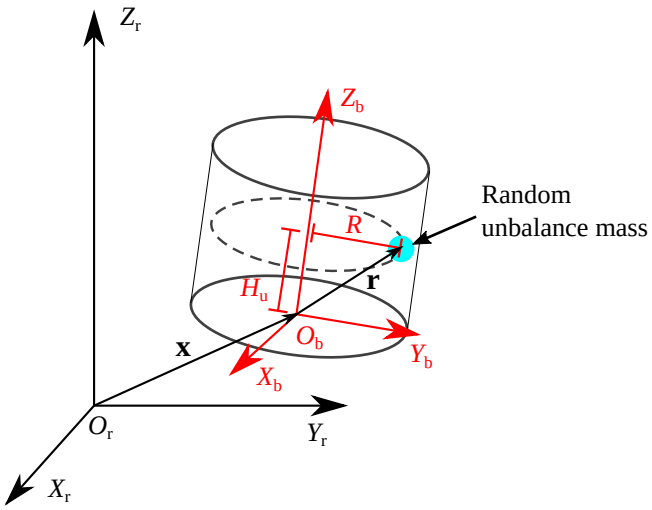

Figure 2 – Schematic representation of the global and local frames. Characterization of the random unbalance through two random variables H_u and M_u.

Stochastic model

In order to incorporate the random unbalance mass into the model, two continuous, uniform and independent random variables are first defined as:

$$\mathscr{U} \sim U[0.5,\ 1.5]\ (\text{kg}) \tag{2}$$
$$\mathscr{H} \sim U[0,\ 0.4]\ (\text{m}), \tag{3}$$

where $\mathscr{U}$ is the random variable that defines the uncertain mass of the unbalance and $\mathscr{H}$ is the random variable that defines to height of the unbalance mass with respect to X_bY_b plane. The intervals for both uniform distributions were defined from experience and experimental observations of a global major manufacturer.

To derive the stochastic model of the WG, the position of the random unbalance with respect to the inertial frame is defined as

$$\mathbf{s}(\mathscr{H}) = \mathbf{x} + \mathbf{R}^{rb}\mathbf{r}, \tag{4}$$

where $\mathbf{x} = \begin{bmatrix} x & y & z \end{bmatrix}^T$ is the position of O_b (the origin of the local frame), written with respect to the inertial frame, and

$$\mathbf{R}^{rb} = \begin{bmatrix} \cos\beta\cos\gamma & -\cos\beta\sin\gamma & \sin\beta \\ \sin\alpha\sin\beta\cos\gamma+\cos\alpha\sin\gamma & -\sin\alpha\sin\beta\sin\gamma+\cos\alpha\cos\gamma & -\sin\alpha\cos\beta \\ -\cos\alpha\sin\beta\cos\gamma+\sin\alpha\sin\gamma & \cos\alpha\sin\beta\sin\gamma+\sin\alpha\cos\gamma & \cos\alpha\cos\beta \end{bmatrix} \tag{5}$$

is the rotation matrix that transform vectors from the local to the global frame. The vector $\mathbf{r} = \begin{bmatrix} R\cos\theta & R\sin\theta & \mathscr{H} \end{bmatrix}^T$ represents the position of the unbalance mass with respect to the local frame, where R is the radius of the drum and θ is the spin angle of the drum with respect to the tank. It is assumed that θ is a known function of time.

In Eq. (4), the vector $\mathbf{s}$ was written as function of the random variable $\mathscr{H}$ to highlight this dependency, although the position vector also depends on $\mathbf{q}$ and θ. Taking the time derivative of Eq. (4), the velocity of the unbalance mass can be written as

$$\begin{aligned} \dot{\mathbf{s}}(\mathscr{H}) &= \dot{\mathbf{x}} + \dot{\mathbf{R}}^{rb}\mathbf{r} + \mathbf{R}^{rb}\dot{\mathbf{r}} \\ &= \dot{\mathbf{x}} - \mathbf{R}^{rb}\tilde{\mathbf{r}}\boldsymbol{\omega} + \mathbf{R}^{rb}\dot{\mathbf{r}} \end{aligned} \tag{6}$$

where $\boldsymbol{\omega}$ is the angular velocity of the local frame $X_bY_bZ_b$ and the tilde superscript represents the skew-symmetric matrix for the cross product operation. The angular velocity can be further decomposed as

$$\boldsymbol{\omega} = \mathbf{B}\dot{\Phi} \tag{7}$$

where $\dot{\Phi} = \begin{bmatrix} \dot{\alpha} & \dot{\beta} & \dot{\gamma} \end{bmatrix}$ and

$$\mathbf{B} = \begin{bmatrix} \cos\beta\cos\gamma & \sin\gamma & 0 \\ -\cos\beta\sin\gamma & \cos\gamma & 0 \\ \sin\beta & 0 & 1 \end{bmatrix}. \tag{8}$$

Substituting Eq. (7) into Eq. (6), the velocity of the unbalance mass can be finally written as

$$\dot{\mathbf{s}}(\mathscr{H}) = \begin{bmatrix}\mathbf{I}_3 & -\mathbf{R}^{rb}\tilde{\mathbf{r}}\mathbf{B}\end{bmatrix}\dot{\mathbf{q}} + \mathbf{R}^{rb}\frac{\partial \mathbf{r}}{\partial \theta}\dot{\theta}, \tag{9}$$

where $\mathbf{I}_3$ corresponds to the 3×3 identity matrix.

The kinetic energy and the gravitational potential energy of the random unbalance mass can now be computed. Using Eq. (9), the kinetic energy becomes

$$\begin{aligned} T_u(\mathscr{U},\mathscr{H}) &= \frac{1}{2}\mathscr{U}\dot{\mathbf{s}}^T(\mathscr{H})\dot{\mathbf{s}}(\mathscr{H}) \\ &= \frac{1}{2}\dot{\mathbf{q}}^T\mathbf{M}_u(\mathscr{U},\mathscr{H})\dot{\mathbf{q}} + \dot{\mathbf{q}}^T\Gamma(\mathscr{U},\mathscr{H})\dot{\theta} + \frac{1}{2}\Upsilon(\mathscr{U})\dot{\theta}^2, \end{aligned} \tag{10}$$

where,

$$\mathbf{M}_u(\mathscr{U},\mathscr{H}) = \begin{bmatrix}\mathscr{U}\mathbf{I}_3 & -\mathscr{U}\mathbf{R}^{rb}\tilde{\mathbf{r}}\mathbf{B} \\ -\mathscr{U}\left(\mathbf{R}^{rb}\tilde{\mathbf{r}}\mathbf{B}\right)^T & \mathscr{U}\mathbf{B}^T\tilde{\mathbf{r}}^T\tilde{\mathbf{r}}\mathbf{B}\end{bmatrix} \tag{11}$$

$$\Gamma(\mathscr{U},\mathscr{H}) = \begin{bmatrix}\mathscr{U}\mathbf{R}^{rb}\frac{\partial \mathbf{r}}{\partial \theta} \\ -\mathscr{U}\mathbf{B}^T\tilde{\mathbf{r}}^T\frac{\partial \mathbf{r}}{\partial \theta}\end{bmatrix}, \tag{12}$$

$$\Upsilon(\mathscr{U}) = \mathscr{U}\left(\frac{\partial \mathbf{r}}{\partial \theta}\right)^T\frac{\partial \mathbf{r}}{\partial \theta}. \tag{13}$$

Using Eq. (4), the gravitational potential energy can be written as

$$V_u(\mathscr{U},\mathscr{H}) = \mathscr{U}\mathbf{g}^T\mathbf{s}(\mathscr{U}), \tag{14}$$

where $\mathbf{g} = \begin{bmatrix}0 & 0 & -9.81\end{bmatrix}$ is the acceleration of gravity. Together, those kinetic and potential energies can be used in the Lagrange equation to derive additional terms, that after being added to the (1), incorporates the effects of the random unbalance in the dynamics of the WG. Considering only the energies of the random unbalance mass, the Lagrange's equation becomes

$$\frac{d}{dt}\left(\frac{\partial \mathbf{T}_u}{\partial \dot{\mathbf{q}}}\right) - \frac{\partial \mathbf{T}_u}{\partial \mathbf{q}} + \frac{\partial \mathbf{V}_u}{\partial \mathbf{q}} = \mathbf{0}, \tag{15}$$

where the dependency of the random variables in the energies was neglected for convenience. After performing the respective derivatives, Eq. (15) becomes

$$\dot{\mathbf{M}}_u\dot{\mathbf{q}} + \mathbf{M}_u\ddot{\mathbf{q}} + \dot{\Gamma}\dot{\theta} + \Gamma\ddot{\theta} - \frac{1}{2}\left[\frac{\partial \mathbf{M}_u}{\partial \mathbf{q}}\dot{\mathbf{q}}\right]^T\dot{\mathbf{q}} - \left[\frac{\partial \Gamma}{\partial \mathbf{q}}\dot{\mathbf{q}}\right]^T\dot{\theta} + \frac{\partial V_u}{\partial \mathbf{q}} = \mathbf{0} \tag{16}$$

Adding Eq. (1) and Eq. (16), the following equation of motion is obtained:

$$\underbrace{(\mathbf{M}+\Delta\mathbf{M}+\mathbf{M}_u)}_{\mathbf{M}_T(\mathbf{q},\theta,\mathscr{U},\mathscr{H})}\ddot{\mathbf{q}} = \underbrace{\frac{1}{2}\left[\frac{\partial(\mathbf{M}+\mathbf{M}_u)}{\partial \mathbf{q}}\dot{\mathbf{q}}\right]^T\dot{\mathbf{q}} - \left(\dot{\mathbf{M}}+\dot{\mathbf{M}}_u\right)\dot{\mathbf{q}} + \mathbf{F}\left(\dot{\theta},\ddot{\theta}\right) - \dot{\Gamma}\dot{\theta} - \Gamma\ddot{\theta} + \left[\frac{\partial \Gamma}{\partial \mathbf{q}}\dot{\mathbf{q}}\right]^T\dot{\theta} + \mathbf{Q} + \mathbf{L} - \frac{\partial(V_{WG}+V_u)}{\partial \mathbf{q}}}_{\mathbf{f}_T\left(\mathbf{q},\dot{\mathbf{q}},\theta,\dot{\theta},\ddot{\theta},\mathscr{U},\mathscr{H}\right)}. \tag{17}$$

Equation (17) represents the nonlinear stochastic model of the WG dynamics. It is important to highlight that $\mathbf{q}$ in Eq. (17) is a random response for the washing machines dynamics since it depends directly on the random variable of the unbalance, $\mathscr{U}$ and $\mathscr{H}$. It consists in a nonautonomous mechanical system since θ is a known function of time. To keep the equation shorter, the right hand-side of Eq. (17) will be called hereafter as $\mathbf{f}_T$. Also, the sum of the mass matrices $\mathbf{M}$, $\Delta\mathbf{M}$ and $\mathbf{M}_u$ will be called from now on as $\mathbf{M}_T$.

STEADY STATE RESPONSE

The steady state response of the WG vibration is now calculated. Therefore, the drum spin speed is considered constant and equals to Ω, so that it is possible to set $\ddot{\theta} = 0$, $\dot{\theta} = \Omega$ and $\theta = \Omega t$ in the equation of motion. The steady state response corresponds to the closed orbit found as the solution of the following periodic boundary-value problem:

$$\begin{cases}\dot{\mathbf{y}}(t) = \mathbf{g}(t,\mathbf{y}(t),\Omega,\mathscr{U},\mathscr{H}), & \text{for } 0 \le t \le T \\ \mathbf{y}(0) = \mathbf{y}(T)\end{cases}, \tag{18}$$

where

$$\mathbf{g}(t,\mathbf{y}(t),\Omega,\mathscr{U},\mathscr{H}) = \begin{bmatrix}\dot{\mathbf{q}}(t) \\ \mathbf{M}_T^{-1}(t,\mathbf{q},\mathscr{U},\mathscr{H})\mathbf{f}_T(t,\mathbf{q},\dot{\mathbf{q}},\Omega,\mathscr{U},\mathscr{H})\end{bmatrix} \tag{19}$$

is the vector field, $\mathbf{y}(t) = \begin{bmatrix}\mathbf{q}^T(t) & \dot{\mathbf{q}}^T(t)\end{bmatrix}^T$ is the state of the system, and $T = \frac{2\pi}{\Omega}$ is the known period of the solution. The first line in Eq. (18) represents the same equation of motion defined in Eq. (17), rewritten in its state space form.

This periodic boundary-value problem can be solved numerically using the Shooting method (Keller, 1968)(Aprille and Trick, 1972)(Chua and Lin, 1975)(Parker and Chua, 1989)(Wagner, 2022). This particular method searches for a specific initial state that, after the equation of motion is integrated along the known period, returns the system to the same initial state and therefore closes the orbit. To find this specific initial state, a residual vector $\mathbf{R}$ must be first defined as

$$\mathbf{R}(\mathbf{y}_0) = \mathbf{y}(T) - \mathbf{y}_0, \tag{20}$$

where $\mathbf{y}_0 = \mathbf{y}(0)$ is the specific initial state that represents the unknowns of the problem. Notice that the final state $\mathbf{y}(T)$ also depends on the specific initial state since it is obtained as the solution of an initial value problem with $\mathbf{y}_0$ as initial conditions. The solution of the periodic boundary value problem is found solving $\mathbf{R}(\mathbf{y}_0) = \mathbf{0}$, which can be done (within some error tolerance) using the Newton-Raphson solver. To integrate the equation of motion from the initial state to the final state, the 4th order Runge-Kutta method was used here. The Jacobian matrix $\frac{\partial \mathbf{R}(\mathbf{y}_0)}{\partial \mathbf{y}_0}$ required by the Newton-Raphson method was also computed numerically using a finite difference method.

It is important for the analysis discussed in this paper to evaluate the periodic solution of the WG vibration for the entire range of spin speeds of the machine. To this end, a sequential continuation was used (Seydel, 1989). The operational spin speed range was first defined from zero to the maximum spin speed, so that $\Omega \in [0,\ \Omega_{\max}]$. A discrete set of spin speed values, $\{\Omega_k\}_{k=0}^{N_s}$, was then defined dividing the operational spin speed range into equally spaced intervals, where $\Omega_k = k\frac{\Omega_{\max}}{N_s}$, and N_s is the number of intervals. The Shooting method was then used to solve the periodic boundary-value problem for each of those discrete values of spin speeds, sequentially, from low to high speeds. The first guessed solution for the periodic solution at a given spin speed Ω_k was set as the previous known solution at a spin speed Ω_{k-1}. The sequential continuation allows the periodic solutions to be define for the same values of discrete spin speed at every new simulation. This is an important requirement to evaluate the probability distribution of the WG vibration discussed in the next section and computed using Monte Carlo simulations. From experience, the sequential continuation should not face any problem while performing this continuation of periodic solutions since no bifurcation point is expected.

For each calculated periodic solution, the displacement of the tank was also calculated at two particular points, the top and bottom position, as illustrated in Fig. 1. The Analysis of the WG dynamics in this paper will be restricted to those points. The top and bottom positions of the tank were chosen because they are common points used to attach accelerometers during vibration tests. This way, a direct comparison between numerical simulations and experimental data becomes possible. From a computed periodic solution, at a given drum's speed and for given samples of the unbalance random variables, the displacements at those two particular points can be calculated using Eq. (4). To this end, let's $\mathbf{r}_t$ and $\mathbf{r}_b$ be the constant position vector of the tank's top and bottom points in the local frame $X_bY_bZ_b$, respectively. Knowing the periodic solution for a given drum's speed and samples of the unbalance random variables, the displacements of those two points can be computed as

$$\mathbf{s}_t = \mathbf{x} + \mathbf{R}^{rb}\mathbf{r}_t \tag{21}$$

$$\mathbf{s}_b = \mathbf{x} + \mathbf{R}^{rb}\mathbf{r}_b \tag{22}$$

where $\mathbf{s}_t$ and $\mathbf{s}_b$ are the position vector of the tank's top and bottom points in the inertial frame, respectively. Notice that $\mathbf{x}$ and $\mathbf{R}^{rb}$ can be defined for each time instant once the periodic solution is known. For those two key displacements, $\mathbf{s}_t$ and $\mathbf{s}_b$, the analysis will be restricted to the peak-to-peak amplitude of the displacement in the X_r direction. Those peak-to-peak amplitudes will be then stored and plotted latter with respect to the drum's speed for each sample of the random variables.

To illustrate this analysis procedure, a periodic solution of the WG computed using the Shooting method is presented in Fig. 3. For this particular simulation, a sample for of the unbalance mass and height was used ($\mathscr{U} = 0.576$kg and $\mathscr{H} = 0.335$m). In Fig. 3a, the translation of the local frame is presented, while its orientation (the Euler's angle) is presented in Fig. 3b. From those curves, it is possible to notice that the motion of the WG occurs mainly in the x and y direction. The approximately constant displacement in the z direction corresponds to the position of the static equilibrium of the WG. For the Euler's angles, there are only small rotations in α and β. From this periodic solution, the displacements at the top and bottom of the tank in the X_r direction were calculated using Eq. (21) and (22), and they are presented in Fig. 3c and Fig. 3d, respectively. For this particular samples of the random variables $\mathscr{U}$ and $\mathscr{H}$, the vibration amplitude at the top of the tank is considerable higher than the one in the bottom. Also, it is possible to see that the maximum displacement at the bottom of the tank has a small delay compared to the maximum displacement at the top. From those curves, the peak-to-peak amplitudes of the top and bottom displacement in the X_r direction can be extracted and stored. Repeating this procedure to all discrete predefined spin speeds, where the periodic solutions were calculated using the Shooting method and the sequential continuation, the peak-to-peak amplitude of the top and bottom displacements in the X_r direction can be plotted with respect to the spin speed, as showed by the in Fig. 3e and Fig. 3f. The red dots represent the peak-to-peak amplitude at 450 RPM. The steady state vibration curve can then be constructed connecting all the dots. Those curves will be used hereafter to compute the probabilistic response of the WG dynamics.

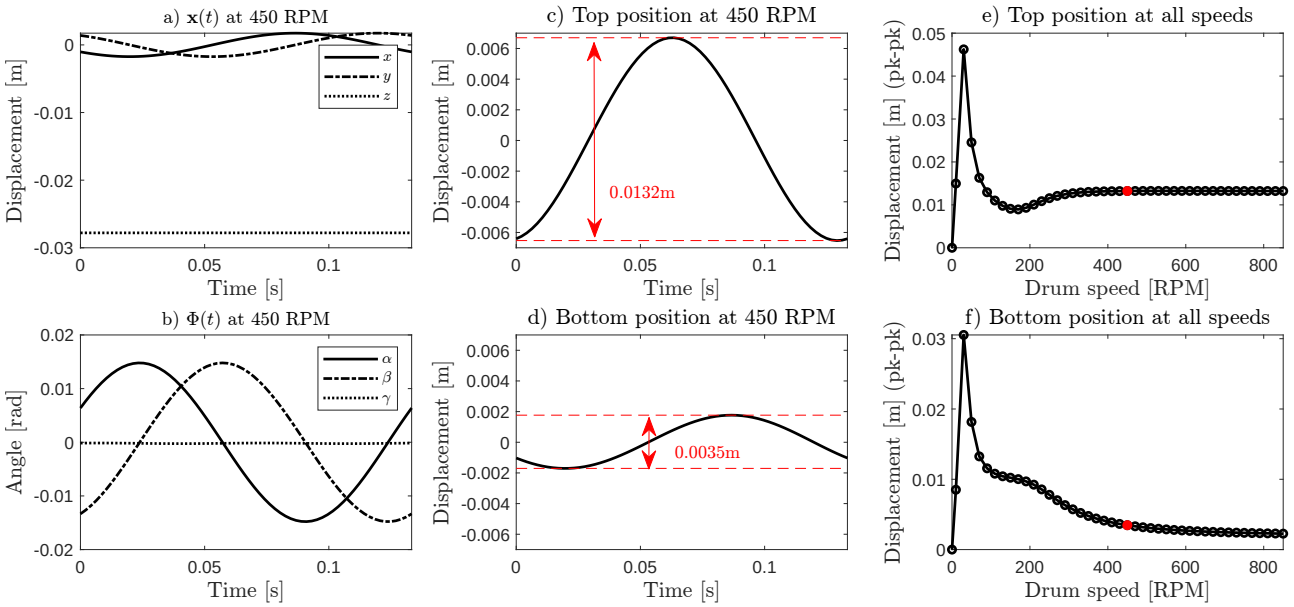

Figure 3 – a) and b) represents the steady state response of the washer vibration. c) and d) are the radial displacements of the tank in the top and bottom position. e) and f) are the pk-pk top and bottom displacements of the tank for different spin speeds.

Before jumping into the probability distribution of the WG vibration, two important comments about its dynamics can already be made from this single simulation run. First, a peak around 60 RPM in the top and bottom radial displacements (Fig. 3e and Fig. 3f) highlights the first critical speed of the WG. The main reason for the existence of this low critical speed is the low resistance imposed by the suspension system in the radial motion of the WG. This low resistance is intentionally designed because the hydraulic balancer requires a supercritical condition of the machine to operates properly (reduce the vibration). It depends on the phase shift between the unbalance mass and the displacement of the WG to accumulate liquid in oposite side of te unbalance. Thus, it is possible to conclude that the hydraulic balanced reduces the vibration for most of the operational speed range of the washing machine. A second comment about the dynamics of WG is the fact that the amplitude of the motion become approximately constant after 400 RPM, characterizing the self-centering effect found in rotors when rotating at supercritical speeds.

MONTE CARLO SIMULATIONS

The unbalance generated by the tangled clothes during a washing cycle is highly random. If the same pieces of clothes are washed twice, the expected unbalance inside the drum, during centrifuge, can be significantly different. Therefore, the unbalanced mass and its relative height with respect to the bottom of the drum had to be set as random variables in the stochastic dynamical model. To analyze the probability distribution of the WG dynamics, Monte Carlo simulations were performed. For each simulation run, a random sample of the unbalance mass and its height was used as inputs to compute the respective steady state vibration curve, as described the in last section. A total of 10000 simulations were performed to estimate the probabilistic distribution of the WG vibration. Using all the computed steady state vibration curves, one histogram was constructed for each discrete spin speed (from 10 to 850 RPM with a 20 RPM increment). To this end, a total of 430000 periodic solutions of the stochastic model had to be calculated, which shows the computational cost of this analysis. With the implemented algorithm, a total of 1.15 s was required, on average, to compute each periodic solution on a personal computer. Figure 4a-f shows some of those histograms (for 150, 350 and 850 RPM). Figure 4g-h shows the concatenation of all histograms using color plots, where the dark red represents the highest probability, while the dark blue represents the lowest.

Some comments about those results are necessary. First, it is possible to notice that the histogram of the top displacements at 150 RPM (Fig. 4a) can be approximate by a uniform distribution. Meanwhile, all the other histograms with spin speed above 200 RPM show a long tail for high vibration amplitudes, an therefore they lose their symmetry with respect to the mean. This characteristic is enhanced as the spin speed increases.

To better understand this changing behavior in the distributions as function of the spin speed, two scatter plots are presented for two spin speeds, 130 and 850 RPM, as shown in Fig. 5. Both plots show the vibration amplitude (peak-to-peak) of the top displacement as function of the unbalance mass and height samples used in the Monte Carlo simulation. Examining Fig. 5a, it becomes clear that the vibration amplitude at low spin speeds (in this case 130 RPM) have a linear dependency on the unbalance mass and it is independent of the unbalance height. Since the top displacement depends

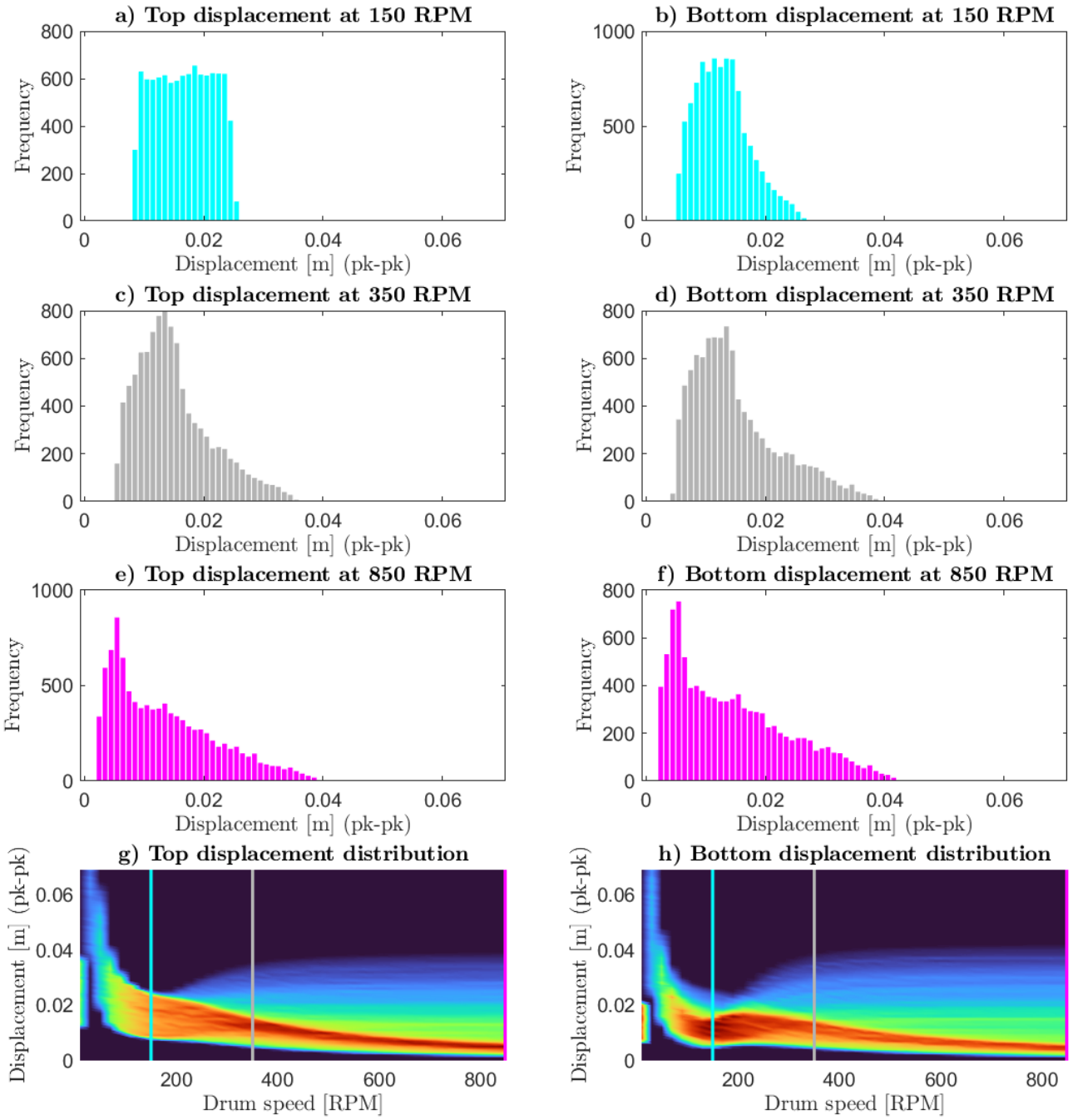

Figure 4 – Probability distribution of the WG peak-to-peak vibration at different spin speeds.

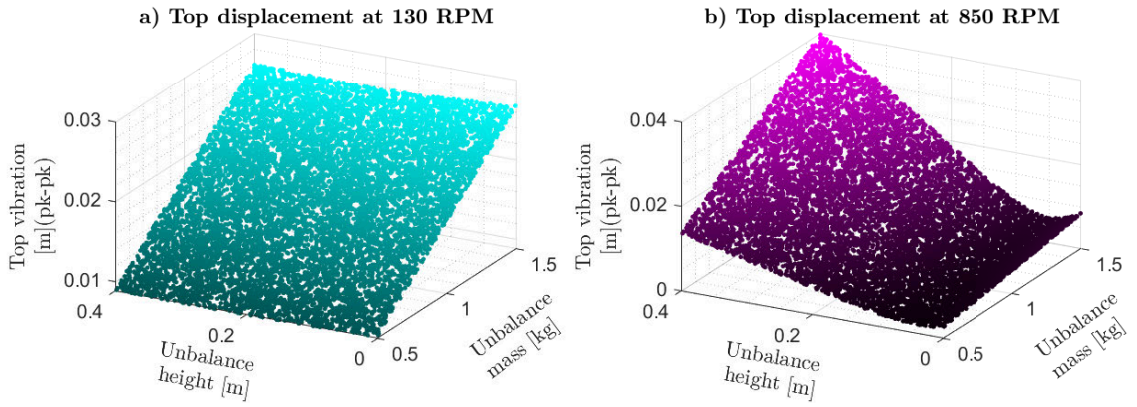

Figure 5 – Scatter plot of the top displacement vibration amplitude (peak-to-peak) as function of the random variables samples.

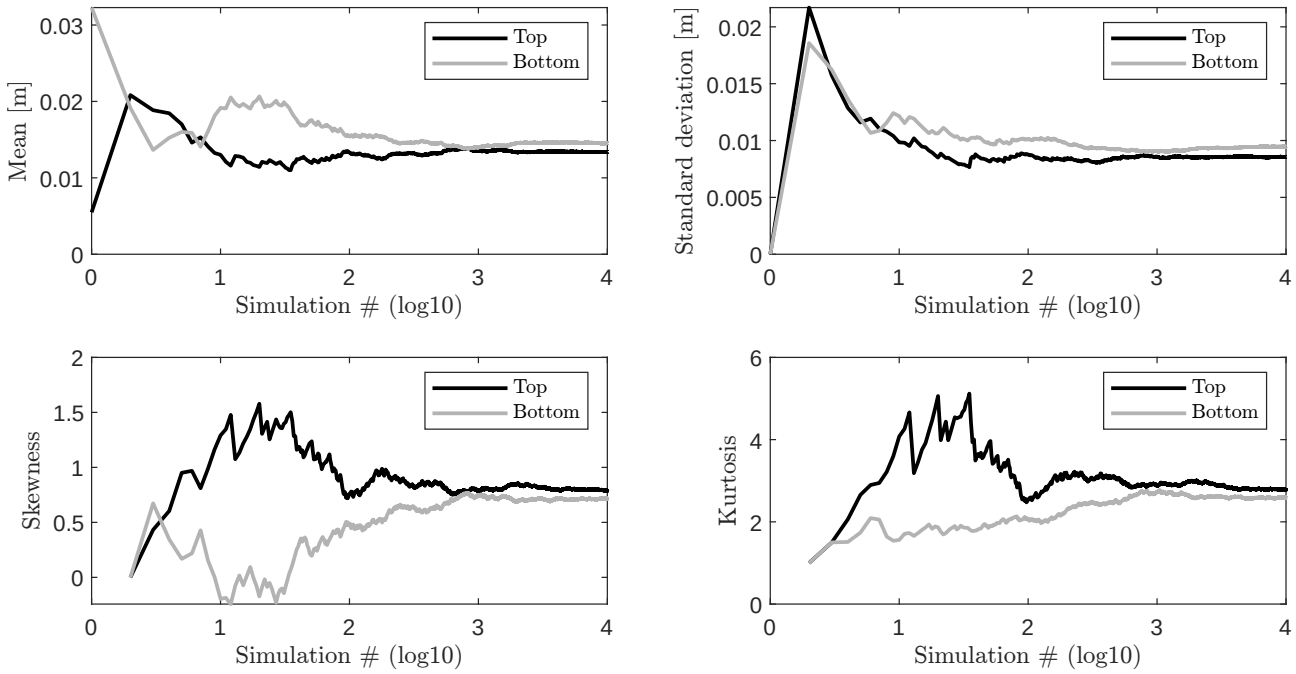

Figure 6 – First four statistical moments of the top and bottom vibration amplitude (peak-to-peak) as function of the number of simulations in the Monte Carlo simulation for a spin speed of 850 RPM.

on only one of the random variables, and because this dependency is linear, the distribution of the displacement follows the same type of distribution of the random variable, in this case, a uniform one. Such behavior drastically changes at high spin speeds, as shown in Fig. 5b. Although an approximately linear dependency in the unbalance mass is still true, the vibration amplitude becomes also dependent on the unbalance height. Apparently, the dependency in the unbalance height is not linear since an increasing in the vibration level is observed when the unbalance height is low ($0 < \mathscr{H} < 0.1$).

To investigate if the number of simulation runs used was large enough to properly characterize the probability distribution of the WG vibration, a convergence analysis of the first four statistical moments of the computed data was performed. The mean, standard deviation, skewness, and kurtosis of the vibration amplitudes were calculated for each spin speed as function of the number of simulations runs. The convergences of all spin speed were similar, and therefore, only the result for 850 RPM is presented in Fig. 6. It was decided to use a logarithm scale for the number of simulations to better visualize the fluctuation of the statistical moments with a small number of samples. From those result, it was possible to confirm that those first four statistical moments reached their convergence with approximately 5000 simulations, which is half of the number used to generate the results in this paper.

CONCLUSIONS

In this paper, the uncertainty in the unbalance mass caused by the unevenly distribution of the clothes in a washing machine was considered for the dynamic analysis of the WG. To this end, the deterministic model proposed by Chen *et al.* (2011) was modified and transformed into a stochastic model. The random unbalance was characterized by two random variables, and the resulting forces in the equation of motion were computed using the Lagrange's equation. The obtained nonlinear equation of motion for the WG dynamics corresponds to a nonautonomous stochastic system, and its steady state solutions (periodic solutions) for different spin speeds were calculated using the Shooting method combined with a sequential continuation. The probability distribution of the WG vibration was approximated using Monte Carlo simulations. From the results, it was observed a changing in the probability distribution of the WG vibration as function of the spin speed. At high speeds, the distributions became less symmetric with a long tail towards the high vibration levels. To better understand these changes in the distributions, a scatter plot of the vibration amplitude as function of the random variables were created. It was possible to conclude that at low spin speed, the vibration depends only on the unbalance mass and not on its height. As the spin speed becomes high, the unbalance height becomes also relevant in the vibration amplitude. At the end, a convergence analysis of some statistical moments of the vibration levels was conducted, and it was used to validated the amount of simulation runs used in the Monte Carlo simulation of this paper.

ACKNOWLEDGMENTS

The authors thank CNPq, CAPES and FAPERJ for the financial support for this research.

REFERENCES

Aprille, T. and Trick, T., 1972. "A computer algorithm to determine the steady-state response of nonlinear oscillators". *IEEE Transactions on Circuit Theory*, Vol. 19, pp. 354–360.

Bae, S., Lee, J., Kang, Y., Kang, J. and Yun, J., 2002. "Dynamic analysis of a automatic washing machine with hydraulic balancer". *Journal of Sound and Vibration*, Vol. 257, pp. 3–18.

Chen, H. and Zhang, Q., 2010. "Stability analyses of a vertical axis automatic washing machine without balancer". *Journal of Sound and Vibration*, Vol. 329, pp. 2177–2192.

Chen, H., Zhang, Q. and Fan, S., 2011. "Study on steady-state response of a vertical axis automatic washing machine with a hydraulic balancer using a new approach and a method for getting a smaller deflection angle". *Journal of Sound and Vibration*, Vol. 330, pp. 2017–2030.

Chua, L. and Lin, P., 1975. *Computer-aided Analysis of Electronic Circuits: Algorithms and Computational Techniques*. Prentice-Hall, Upper Saddle River, NJ.

Conrad, D. and Soedel, W., 1995. "On the problem of oscillatory walk of automatic washing machines". *Journal of Sound and Vibration*, Vol. 188, pp. 301–314.

Cursi, E. and Sampaio, R., 2015. *Uncertainty Quantification and Stochastic Modeling with Matlab*. Elsevier, Oxford, UK.

Keller, H., 1968. *Numerical Methods for Two-point Boundary-value Problems*. Blaisdell.

Lima, R. and Sampaio, R., 2018. "What is uncertainty quantification?" *Journal of the Brazilian Society of Mechanical Sciences and Engineering*, Vol. 40, pp. 1–8.

Parker, T. and Chua, L., 1989. *Pratical Numerical Algorithms for Chaotic Systems*. Springer, New York, USA.

Seydel, R., 1989. *From Equilibrium to Chaos: Practical Bifurcation and Stability Analysis*. Elsevier, New York, USA.

Wagner, G., 2022. *An excursion in the dynamics of flexible beams: from modal analysis to nonlinear modes*. Ph.D. thesis, Graduate Program in Mechanical Engineering, PUC-Rio, Rio de Janeiro, Brasil.

RESPONSIBILITY NOTICE

The authors are the only responsible for the printed material included in this paper.